Gauche- Ethyl Alcohol: Laboratory Assignments and Interstellar Identification

J. C. PEARSON

Jet Propulsion Laboratory, Mail Stop 83-301, 4800 Oak Grove Dr.

Pasadena, CA 91109-8099

K. V. L. N. SASTRY

Department of Physics, University of New Brunswick

Fredericton, New Brunswick, E3B 5A3 Canada

ERIC HERBST[1] AND FRANK C. DE LUCIA

Department of Physics, The Ohio State University, Columbus, OH 43210-1106

Also: Department of Astronomy, The Ohio State University, Columbus, OH 43210-1106

Friday, August 02, 1996

Abstract

Ethyl alcohol (ethanol) is known to possess a pair of closely-spiced excited torsional substates (*gauche*+, *gauche*-) at an energy of approximately 5'/ K above the ground (*trans*) torsional substate. We report an extended analysis of some *gauche*- - *gauche*+ Q branch (ΔJ =-O) transitions with a three-substate fixed frame axis method (IFAM) Hamiltonian. Our approach accounts for complex *trans-gauche* interactions for the first t imc. In addition, we are able to obtain intensities for perturbed rotational transitions, and to determine the. *trans* to *gauche*+ separation to be 11 85399.] MHz. A complete ground state rotational-torsional partition function accounting, for the previously neglected *gauche* substates is presented. Based on our analysis, a total 01'14 U-lines obtained towards Orion-KL can now be assigned to *gauche* substates of ethanol. Analysis of these lines yields a rotational temperature of 223 K and a total (*trans* + *gauche*) column density of 2.8×10^{15} cm^{-2}. The column density is in reasonable agreement with the recent value of: 1×10^{15} cm^{-2} for *trans*- ethanol by Ohishi et al. although there is some disparity in the rotational temperatures. Eight additional 11-lines in the literature are assigned to transitions of *gauche*-ethanol.

Subject Headings: ISM: molecules - line: identification - molecular data - molecular processes - radio lines: lSM

I. Introduction

Ethyl alcohol (ethanol) has been observed in several warm dense interstellar clouds. It was initially detected in Sgr B2 by Zuckerman et al. (1975) and later detected in W51M by Millar et al. (1988) with a large fractional abundance of 10^{-7}. Ethanol has also been reported towards Orion-KL, by Turner (1989, 1991) and (tentatively) by Ziurys & McGonagle (1991). The most recent detection towards Orion-KL, and the most convincing, has been made by Ohishi et al. (1995). These authors detected four lines of ethanol and obtained a column density $N \approx 1 \times 10^{15}$ cm^{-2} and a rotational temperature of $\approx$ 70 K. Also quite recently, a large number of submillimeter transitions have been detected in the Hot Core G34.3 +0.15, and a rotational temperature of 125 K and a column density of 2.0×10^{15} cm^{-2} derived (Millar, Macdonald, & Habing 1995). The recent observations suggest that ethanol is primarily localized in hot core regions with gas densities of 10^6-10^8 cm^{-3} and temperatures near or in excess of 100 K. Although several mechanisms for forming ethanol in the gas phase have been proposed (Millar et al. 1988), its large abundance in hot cores suggests a major role for dust chemistry (Charnley et al. 1995). In these sources, it is probable that ethanol or a suitable precursor is formed on the surfaces of dust particles during a previous colder era. Once star formation begins, the regions warm, evaporating the ethanol or precursor (Caselli, Hasegawa, & Herbst 1993).

The rotational spectrum of ethanol is complicated and often perturbed by internal rotation (torsional) motions, especially by the motion of the hydroxyl (OH) proton which leads to *trans* and *gauche* substates. In the ground vibrational state, the *trans* substate is the lowest in energy; rotational transitions in this substate are the ones previously observed in the interstellar medium. The rotational spectrum of ethanol has been the subject of several previous laboratory investigations; summaries are given in Pearson et al. (1995, 1996). In our first paper on the ground vibrational state spectrum of ethanol (Pearson et al. 1995), we measured and analyzed a large number of millimeter-wave and submillimeter-wave

rotational transitions in the *trans* substate, while in our second paper (Pearson et al. 1996) we measured and analyzed a large number of transitions in the two closely-spaced *gauche* states (*gauche*+ and *gauche*-), which lie only 57 K above the *trans* substate and are easily excited in warm interstellar regions, although no identifications of interstellar *gauche*-ethanol have been previously reported, to the best of our knowledge. The rotational transitions in the *gauche* substates consist of transitions within each substate and transitions which cross from one substate to the other.

Previous laboratory investigations of rotational transitions in the ground vibrational state of ethanol have treated the *trans* and two *gauche* substates as non-interacting, but such analyses are only successful for a limited range of the quantum numbers J and K_a (Pearson et al. 1995, 1996) due to strong *trans-gauche* interactions outside this range. In this paper, we report the first combined *trans*- and *gauche*- ethanol ground state analysis, the precise *trans* to *gauche* energy difference, and laboratory spectra of four often perturbed c-type ($\Delta K_a = \pm 1$, $\Delta K_c = 0$) *gauche*- to *gauche*+ Q branches ($\Delta J = 0$) and their perturbation allowed x-type ($\Delta K_a = 0$, $\Delta K_c = 0$) counterparts.

Our previous analysis of *gauche*-ethanol and our current combined *trans-gauche* analysis have enabled us to assign and analyze 14 U-lines in the 97.5 - 98.0 GHz region as belonging to three different Q branches between the *gauche* torsional substates of ethanol. The U-lines were observed in Orion-KL and reported by Ohishi et al. (1988) as part of a search for the PS radical. These transitions have line widths on the order of 3 km s^{-1}, which is consistent with the quiescent portions of the source - the Hot Core and the Compact Ridge, the latter known for its oxygen-rich organic molecules (Blake et al. 1987). Ohishi et al. (1988) speculated that the U-lines were high-lying but ruled out methanol and its ^{13}C isotopomer as the carriers. Although the majority of the U-lines can be assigned directly from the results of Pearson et al. (1996), there are some which lie above the J and K_a limits of that analysis. These lines show significant perturbations with the *trans* substate; as a result line strength and transition frequency calculations require the model of

the entire ground state presented in this paper. With intensities generated by our model, we can determine the ethanol column density and rotational temperature in Orion-KL. We also propose assignments of eight other previously reported U-lines to *gauche* ethanol Q branch transitions.

2. Theory

Ethanol is a prolate asymmetric top ($\kappa = -0.92$) with two large amplitude internal motions, the three-fold internal rotation of the protons of the methyl group, and the asymmetric internal rotation of the hydroxyl proton. The methyl internal rotation has C_3 group symmetry, which results in A and E substates with A to A and E to E selection rules. The three-fold-symmetric (V_3) barrier for the methyl internal rotation was determined to be 1173.7 cm^{-1} (Pearson et al. 1995) and 1331 cm^{-1} (Kakar & Quade 1980) in the *trans* and *gauche* substates of the ground vibrational state, respectively. Since these barriers are rather high, transitions of the ground state A and E components occur with less than 1 h4117 separation. The A/E splittings can often be resolved in the *trans* substate, but can rarely be resolved in the *gauche* substates. in the submillimeter region, methyl torsional splittings are almost never resolved and are effectively averaged by any measurements, Any resolved methyl torsional splittings have been averaged in this treatment of ethanol.

The potential for the motion of the (J] 1 proton has a global minimum (the *trans* well) which corrc.spends to the hydroxyl proton lying in the CCO plane. Two secondary minima (the *gauche* wells) occur when the proton lies approximately 120° from the *trans* minimum (Pearson et al. 1996). Figure 1 silo\\'s the potential based on some recent work of Su & Quade (1996). The energy difference between the *trans* and *gauche* minima is due to the. departure from perfect three-fold symmetry. The plane of symmetry containing the *trans* minimum can be used to describe the symmetry of torsional wave functions with the C_s symmetry group. Solution of the torsional wave equation results in a series of wave

functions which are symmetric (c) or antisymmetric (o) about the. ('('() plane of symmetry and can be labeled by the number of nodes. Since the barrier is predominantly three-fold, each torsional state is divided into three substates. The lowest energy wave function, c_0 01" *trans*, **has** no **nodes,** is symmetric, and peaks in amplitude at the *trans* minimum. The next two wave functions have one node and comprise a symmetric (c_1 or *gauche*+), antisymmetric (o_1 or *gauche*-) closely--s]xlccd pair with amplitude peaks at the *gauche* potential minima. Ground stale. torsional wave functions computed with the potential of Su & Quade (1996) are shown in 1 'igure 2. These wave functions are sig nifcantly less localized than those calculated from the previous potential of Kakar & Quade (1980), which contains a slightly higher barrier.

The selection rules determined by the C_s group allow a- and b-type transitions between substates of the same. symmetry and c-type transitions between substates of different symmetries. As a result, a- and b type transitions are formally allowed within each torsional substate and between *trans* and *gauche*+, while. c-type transitions are allowed bet ween *gauche*+ and *gauche* - and *trans* and *gauche*-. The reported dipole mome.ills for ethanol are give.n in matrix form in Table I. I n the *trans* substate, the b-component of the dipole moment dominates, while the a-component is quilt small. In the *gauche* torsional substates, the a-component of the dipole is large and the b-component smal r. It should be noted that no *trans* a-type or *gauche* b-type transitions have been observed in the. absence of large level mixing. The line strengths predicted from the dipole moment components reported for these states should lend to observation of transitions; however, these transitions have not been detected in spectrometer systems with high sensitivity, suggesting that the effective transition moments may be significantly smaller than previously reported. It should also be noted (hat the dipole components were determined using analyses which did not include many important interactions among the substates of t i ne ground vibrational state. Symmetry-al lowed transit ion moments between the *trans* and *gauche* substates are

not known and are listed as "not available" in Table 1. The *trans* to *gauche* transition moments are expected to be small due to limited torsional overlap between these substates.

We have previously discussed a suitable Hamiltonian for OH torsional motion in ethanol and its interaction with the overall rotational motion (Pearson et al. 1996). The Hamiltonian **11,** derived and applied by Quade and co-workers (Quade & Lin 1963; Quade 1X6, 1967; Knopp & Quade 1968), can be divided into three terms:

$$\mathbf{H} = \mathbf{H}_R + \mathbf{H}_{TR} + \mathbf{H}_T \qquad (1)$$

Here $\mathbf{H}_R$ is the rigid-body rotational Hamiltonian with centrifugal distortion, $\mathbf{H}_T$ is the torsional Hamiltonian, and $\mathbf{H}_{TR}$ is the torsion-rotation interaction. A variety of steps lead to an effective Hamiltonian which contains operators similar to those used in treating Coriolis and Fermi interactions between vibrational states. This effective Hamiltonian H to second order in angular momentum is given by the expression

$$\begin{aligned} H_R &= A^{(\sigma)}P_a^2 + B^{(\sigma)}P_b^2 + C^{(\sigma)}P_c^2 + F^{(\sigma)}(P_aP_b + P_bP_a) \\ H_{TR} &= D^{(\sigma^1,\sigma^2)}(P_bP_c + P_cP_b) + E^{(\sigma^1,\sigma^2)}(P_cP_a + P_aP_c) + F^{(\sigma^1,\sigma^2)}(P_aP_b + P_bP_a) + \\ &\quad M^{(\sigma^1,\sigma^2)}P_c + N^{(\sigma^1,\sigma^2)}P_b + Q^{(\sigma^1,\sigma^2)}P_a + R^{(\sigma^1,\sigma^2)}(P_b^2 - P_c^2) + S^{(\sigma^1,\sigma^2)}P_a^2 \\ H_T &= \Delta E^{(\sigma)} \end{aligned} \qquad (2)$$

where the P_i are the components of angular momentum along the principal axes (i = a,b,c), and the spectroscopic constants contain superscripts σ which refer to torsional substate. The procedure is referred to as the fixed framework axis method (1FFAM). In the FFAM formulation, all the H_{TR} terms connect two different torsional substates, so that the spectroscopic constants have two superscripts $\sigma^1 \neq \sigma^2$. An H_R term exists for each substate; setting $F^{(\sigma)}$ to zero for one of the substates defines the axis system of the entire molecule as the effective principal axes of that substate (*trans* in this case). The H_T terms do not contain kinetic and potential energy expressions relating to torsional motion; rather they are simply parameters which define the energies of the *gauche* substates with respect to the *trans* substate. In addition to expanding the H_R terms to include higher order angular momentum terms, all the operators off diagonal in torsional substate can be

expanded (Pearson et al. 1996) in order to help account for the higher order effects of the torsion and torsion-rotation interactions which are only approximately treated in this Hamiltonian formulation.

The C_s symmetry group dictates which of the H_{TR} terms possess non-zero off-diagonal matrix elements between which set of substates, as discussed in our earlier work (Pearson et al. 1996). Here we briefly discuss the inclusion of these terms for *trans-gauche* interactions. Their effect is to produce perturbations from normal asymmetric top energy level patterns, selection rules, and intensities. In addition to possessing a dependence on torsional substate, the off-diagonal matrix elements also depend on the angular momentum quantum numbers. Since the total angular momentum J is a good quantum number, H_{TR} connects only those pairs of rotational levels in different torsional substates with the same total angular momentum J. To understand the dependence of non-zero matrix elements on the "pseudo" quantum numbers K_a and K_c, let us first consider ethanol to be a prolate symmetric top so that K_a is a real quantum number. In this limit, non-zero off-diagonal elements for the *trans-gauche* interactions exist for $\Delta K_a = 0, \pm 1, \pm 2$. The true asymmetric top functions, however, contain many different K_a quantum numbers (the designated quantum numbers K_a and K_c only refer to the most important prolate and oblate basis functions) so that *trans-gauche* interactions can occur when K_a changes by any amount. For interactions between the *trans* and the *gauche+* substates, K_c must change by an even amount ($\Delta K_c = 0, \pm 2$ in the oblate symmetric top limit) and for interactions between the *trans* and gauche- substates, K, must change by an odd amount ($\Delta K_c = \pm 1$ in the oblate symmetric top limit). Unfortunately, these rules do not hold in all instances, since the *gauche* substates are often mixed (Pearson et al. 1996). Despite this great complexity, the analysis of interactions is aided by the general fact that the strongest interactions between pairs of rotational levels involve the smallest changes in K_a and the most closely spaced energy levels computed without interactions (this is quantified in the

next section). In particular, when two series of energy levels, each denoted by K_a and K_c are plotted vs J, it can be seen that interactions are strongest at so-called "level crossings."

In our earlier work on the spectra of the *gauche* torsional substates, we included only interactions between those two substates. In this paper, we have utilized a ful three-substate formulation, which is the first time to the best of our knowledge that three states including two of the same symmetry (*trans* and *gauche+*) have been analyzed with the FAM method. Although our more complex analysis does not yet allow us to analyze a of the measured transitions, i has facilitated a considerable extension in the J and K_a range of our earlier work

3. Analysis

During the course of our investigations on the millimeter-wave and submillimter-wave spectrum of ethanol (Pearson et al. 1995, 1996; this work), laboratory measurements were undertaken using five different spectrometer systems. The details of these spectrometer systems can be found elsewhere (Helminger, Messer, & De Lucia 983; Booker, Crownover, & De Lucia 1988; King & Gordy 1953; Friedl et al. 1995). A number of additional 12-26 GHz transitions have been assigned from a survey reported by Michielsen-Effinger (1962).

Our ground vibrational state data set now contains approximately 3500 measured transitions, of which approximately 1600 have appeared previously in the literature (Pearson et al. 1995, 996). The analyzed transitions lie between 8 and 652 GHz and cover J and K_a range of 50 and 7, respectively. The present three-state model fits all 3500 transitions with a root-mean-square deviation of 400 kHz, with the majority fitting to near experimental accuracy (50-100 k Hz). Despite a few remaining problems, the current analysis has successfully fit many transitions shifted more than 1 GHz by previously neglected *trans-gauche* interactions. Although our spectroscopic work is incomplete, we are currently able to report a variety of astronomically interesting and perturbed *gauche- to*

gauche+ spectral branches. These branches were partially analyzed in our previous wink, but now we have been able to analyze these branches to a much higher J quantum number. A complete list of spectral transitions along with a comprehensive analysis will appear later.

We have divided the newly analyzed spectral lines into two tables. Table 2 contains *gauche*- - *gauche*+ K_a= (), 1 and K_c= J ^cQ (ΔJ= O, ΔK_a=+1, ΔK_c=0) branches along with perturbation allowed ^xQ (ΔJ=0, ΔK_a= O, ΔK_c= O) transitions between the same levels where seen. '1'able 3 contains *gauche*- - *gauche*+ K_a= 1, 2 and K_c= J- 1 ^cQ branches along with perturbation allowed ^xQ transitions between the same levels where seen. Some Of the lower J lines (J<30) in the tables were also analyzed with our previous two stale analysis (Pearson et al. 1996). These two tables include. the quantum numbers, the measured frequencies, the measurement uncertainties, the observed minus calculated frequencies, the logarithm of the 300 K intensities in units of nm^2·MHz, and the lower state energies. in the tables, the *gauche*+ state is denoted by t= O and the *gauche*- state by t= 1. A significant number of the.sc transitions involve. highly perturbed levels and are denoted in the note column with a gg for a *gauche*+*gauche*- perturbation Or tg for a *trans gauche* perturbation. Note that although the designated tg perturbations onset at high J, such interactions are important at lower J as well.

To provide a feel for the *trans gauche* (tg) interactions involve.d in the tllrcc-state analysis, we have shown *trans-gauche* level crossings for *gauche* J(0, J) and J(1,J) levels in 1 'igure 3, and *trans-gauche* level crossings for *gauche* J(1,J-1) and J(2,J - 1) levels in 1 'igure 4. The *gauche* levels in 1 'igure 3 are the energy levels which are connected by the transitions in 'l'able 2 while the *gauche* levels in 1 'igure 4 are the levels connected by the transitions listed in Table 3. The *gauche* levels, plotted as a function of J with respect to the lowest level 01 the four depicted, are shown as the horizontal or nearly horizontal lines. *Gauche-gauche* (gg) interactions, which peak at J= 13 and J= 18 are especially noticeable in 1 'igure 4. '1'0 illustrate possible interact ions with *trans* levels, the energies of selected *trans* levels defined by K_a are also shown. These energies increase more rapidly as functions of

J and cross the *gauche* levels; at the crossings interactions are noticeable even if the K_a values of the *gauche* and *trans* levels differ by wide amounts. The (+) and (-) shown after the labeling of the *trans* levels refer to the symmetry of the interacting *gauche* substate. The strength 01 the interaction between levels that cross in the absence Of torsion - rotational interaction decreases about one order of magnitude for each quantum of K_a difference, with the ΔK_a=-2 interactions being about 3 GHz. and ΔK_a= 5 interactions being about 3 MHz.

In Tables 2 and 3, the strengths of the lines are denoted by the logarithm Of the intensit y I at temperature 'I', which is given by the formula

$$I(T) = (8\pi^3 / 3hc)\nu_{ba}\, {}^{x}S_{ba}\mu_x^2 \left[e^{-E''/kT} - e^{-E'/kT}\right] \frac{1}{Q_{rs}}, \qquad (3)$$

where ν_{ab}, ${}^{x}S_{ab}$, μ_x, E", E', and Q_{rs} are, respectively, the transition frequency, the line strength including the. 'g' degeneracy factor, the transition dipole component along the relevant axis, the lower and upper slate energies, and the rotational partition function. This unit of intensit y, based on the integral 01 II ie corrected absorption cross section over the spectral line shape, is thoroughl y defined in the JPL Submillimeter, Millimeter, and Microwave Spectral Line Catalog (Poynter & Pickett 1985; Pickett et al. 1996; available online at ht tp://spec.jpl. nasa .gov) The intensities in Tables 2 and 3 are based on the transition moments in 'J'able 1, with all unk nown values assumed to be zero.

In order to obtain an accurate partit ion function, the *trans* to *gauche*+ tunneling frequency, or energy difference, must be k nown. This parameter is determined by the location of perturbations between *trans* and *gauche* levels and by the frequencies of several perturbation-allowed *trans* to *gauche* transitions. The best value for the energy difference between the rotationless *trans* and *gauche*+ substates is 1185399.1 (5.0) MHz, or 39.54 066 (17) cm^{-1}. Although this number does not represent a final value since our analysis is as yet in complete, it is certainly sufficiently accurate to calculate column densities and rotational temperatures. T'able 4 contains Q_{rs} values for a variety of

temperatures, calculated with an explicit sum over all states of the ground vibrational state (*trans* and *gauche*) up to J=50. An analytical approximation to the three-substate Q_{rs}, accurate to within a few % and based on the classical (continuous) approximation, is given by the expression

$$Q_{rs}(T) = T^{3/2}\{3.27 + 3.34\exp(-56.89/T) + 3.34\exp(-61.54/T)\}. \quad (4)$$

Interestingly, nuclear spin plays no role here because there is only one hydroxyl proton, so that Pauli Exclusion Principle considerations do not pertain, as long as motions in the remainder of the molecule cannot act in concert with the hydroxyl proton to return the molecule to an indistinguishable configuration.

4. Astronomical Assignments

The U-lines from Ohishi et al. (1988) believed to be due to ethanol are given in Table 5. The observed U-line frequency, measured (laboratory) rest frequency, T^*_A, Δv, $\mu^2 S$, lower state energy, upper state energy, and quantum assignment are also given. The method used here for determining the total column density N, discussed by Blake et al. (1986) and Turner (1991), contains the assumption that the emission source is optically thin and characterized by a single excitation temperature T_{rot}. In this approximation, the logarithm of the upper state column density N_u divided by the upper state degeneracy g_u can be plotted vs. the upper state energy E_u/k in the following manner:

$$\log_{10}(N_u/g_u) = \log_{10}\left(\frac{3kW}{8\pi^3 \nu_{ab} S_{ab}\mu^2}\right) = \log_{10}\left(\frac{N}{Q_{rs}}\right) - \frac{E_u}{k}\left(\frac{\log_{10}(e)}{T_{rot}}\right), \quad (5)$$

so that the slope $(-\log_{10}(e)/T_{rot})$ and intercept $\log_{10}(N/Q_{rs})$ contain the excitation temperature T_{rot} and the total column density N divided by partition function Q_{rs},

respectively. Here W is the integrated line intensity which, with an assumed beam efficiency of 100%, is estimated to be T_A times the velocity linewidth Δv, and the other parameters are the same as in equation (3). Figure 5 is the plot, known as a rotation diagram, for the transitions in Table 5. The clearly blended line (U97597.8) has been excluded from the analysis. The U97536.7 blend has been included as an intensity weighted sum of the two transition involved.

From the 12 data points (11 single lines and 1 pair), we derive a best fitting rotational temperature of 223 (+66/-35) K, and a column density of $2.8(+3.9/-1.7) \times 10^{15}$ cm^{-2}. Both of these numbers can be compared with the recent values of Ohishi et al. (1995), determined from an analysis of four low-lying lines of *trans*-ethanol. These authors obtained a rotational excitation temperature of 70 K, which is significantly lower than ours. Using this temperature to determine the ratio of the total to *trans* partition functions, we calculate that their column density should be multiplied by a factor of ≈ 2 to obtain a total column density. The resulting total column density of 2×10^{15} cm^{-2} is in good agreement with our value. Although the rotational temperature we obtain is not in good agreement with that of Ohishi et al. (1995), it is in better agreement with an earlier value of Turner (1991) who, if a-type transitions are neglected, determined a rotational temperature of 216 K for *trans*-ethanol.

It is interesting to speculate on whether the 11-lines assigned here belong to the 110[Core or to the Compact Ridge. The latter source is known for oxygen-containing organic molecules, although many molecules in this source have lower rotational temperatures than we determine for *gauche*-ethanol. It seems clear that the lines seen by Ohishi et al. (1995) do stem from the Compact Ridge. Assuming ethanol to lie in either the Hot Core or the Compact Ridge, its fractional abundance with respect to 11> can be estimated to be 10^{-8}, a number equivalent to that determined for other sources.

Table 6 contains a second list of U-lines reported by Lovas (1991) which may be attributable to the *gauche* ethanol Q branch transitions presented in this paper. In addition

to the U-lines and relevant laboratory ethanol frequencies, Table 6 includes assignments, astronomical sources, T_R/T_A and the original references for the U- ines.

5 Summary

This is the third paper in a series on the laboratory millimeter-wave and submillimeter-wave spectrum of ethanol. In this paper, we introduce for the first time an analysis in which interactions among the three torsional substates of the ground vibrational state are considered. Without a consideration of these interactions, previous separate analyses of the lowest *trans* substate (Pearson et al. 1995) and the excited *gauche* substates (Pearson et al. 1996) are limited to a restricted range of angular momentum quantum numbers. Although our three-substate analysis is currently capable of fitting 3500 transitions to a root-mean-square deviation of 400 kHz, we anticipate that future improvements will permit us to fit the laboratory data to near experimental accuracy (50-100 kHz). At the current stage of development, we have successfully analyzed four often badly perturbed *gauche-* - *gauche+* Q branches. In addition, we have been able to predict line positions and calculate intensities for a large number of other perturbed transitions. Finally, the *trans-gauche+* energy difference of 1185399.1(5.0) MHz has been accurately determined.

From our measurements and calculations, we have assigned 14 astronomical U-lines in the 97.5 to 98.0 GHz region of the spectrum, seen in the direction of Orion-KL, to transitions between the two *gauche* substates of ethanol. Analysis of these lines indicates a high rotational temperature (223 K) and a large ethanol column density (2.8×10^{15} cm^{-2}) representative of a hot core-type source, although whether the lines originate in the actual Hot Core or the Compact Ridge has not been determined. The rotational temperature is approximately a factor of three larger than that determined using low-lying transitions in

trans-ethanol by Ohishi et al. (1995) in the Compact Ridge. Perhaps one temperature does *not* describe the rotational-torsional distribution of ethanol towards Orion-KL.

Whatever its temperature, the large abundance of ethanol cannot be accounted for purely by gas-phase chemistry, indicating yet again the importance of dust chemistry in the formation of saturated interstellar organic molecules. We have also proposed assignments for 8 additional interstellar U-lines to our recently analyzed *gauche*- to *gauche*+ Q branch ethanol transitions. Other tentative assignments of U-lines in Sgr B2 and other sources to *gauche*-ethanol based on our original work (Pearson et al. 1996) have been communicated to us by Millar (1996) and Ohishi (1996).

Previous determinations of interstellar column densities for ethanol have, to the best of our knowledge, ignored the *gauche* substates. Since these substates comprise two thirds of the ground vibrational state energy levels, they must be considered in column density determinations unless the excitation temperature is considerably lower than the 57 K excitation of the *gauche*+ substate. Because ethanol appears to be abundant only in warmer regions of molecular clouds, this exception is unimportant .

The portion of this work performed at the Jet Propulsion Laboratory, California Institute of Technology, was done under contract with the National Aeronautics and Space Administration. We would like to thank NASA for their support of laboratory astrophysics at the Ohio State University and the Ohio State University Supercomputer Center for the award of time On their Cray YMP8 computer. K. V. L. N. Sastry thanks Deutscher Akademischer Austrauschdienst (DAAD) for financial support during his stay in Giessen, Germany. The laboratory work in Giessen was supported by the Forschungsgemeinschaft and Fonds der Chemischen Industrie.

REFERENCES

Blake, G. A., Sutton, E. C., Masson, C. R., & Phillips, T. G. 1986, ApJS, 60, 357

.....---..... 1987, ApJ, 315, 621.

Booker, R. A., Crownover, R., & De Lucia, F. C. 1988, J. Mol. Spectrosc., 128, 62.

Caselli, P., Hasegawa, T. I., & Herbst, E. 1993, ApJ, 408, 548.

Charnley, S. B., Kress, M. E., Tielens, A. G. G. M., & Millar, T. J. 1995, ApJ, 448, 232.

Cohen, E. A. 1995, private communication.

Friedl, R. R., Birk, M., Oh, J. J., & Cohen, E. A. 1995, J. Mol. Spectrosc., 170, 383

Helminger, P., Messer, J. K., & De Lucia, F. C. 1983, Appl. Phys. Lett., 42, 309.

Kakar, R. K., & Quade, C. R. 1980, J. Chem. Phys., 57, 4060.

King, W. C., & Gordy, W. 1953, Phys. Rev., 90, 319.

Knopp, J. V., & Quade, C. R. 1968, J. Chem. Phys., 48, 3317.

Kutner, M. L., Machnik, D. E., Tucker, K. D., & Dickman, R. L. 1980, ApJ, 242, 541.

Lovas, F. J. 1991, J. Phys. Chem. Ref. Data, 21, 181.

Michielsen-Effinger, J. 1962, Bull. Acad. Roy. Belg., 48, 438.

Millar, T. J. 1996, private communication

Millar, T. J., Olafsson, H., Hjalmarson, A., & Brown, P. D. 1988, A&A, 205, L5.

Millar, T. J., Macdonald, G. H., & Habing, R. J. 1995, MNRAS, 273, 25.

Ohishi, M. 1996, private communication

Ohishi, M. et al. 1988, ApJ, 329, 511.

Ohishi, M., Ishikawa, S.-I., Yamamoto, S., Saito, S., & Amano, T. 1995, ApJ, 446, L43

Pearson, J. C., Sastry, K. V. L. N., Winnewisser, M., Herbst, E., & De Lucia, F. C. 1995, J. Phys. Chem. Ref. Data, 24, 1

Pearson, J. C., Sastry, K. V. L. N., Herbst, E., & De Lucia, F. C. 1996, J. Mol. Spectrosc., 175, 246.

Pickett, H. M., Poynter, R. L., Cohen, E. A., Delitsky, M. L., Pearson, J. C., &

Müller, H. S. P. 996, Submillimeter, Millimeter, and Microwave Spectral ,ine Catalog, JPL Publication 80-23, Rev. 4

Poynter, R. ., & Pickett, H. M. 1985, Appl. Optics, 24, 2235

Quade, C. R. 1966, J. Chem. Phys., 44, 2512.

----------. 1967, J. Chem. Phys., 47, 1073.

Quade, C. R., & Lin, C. C. 963, J. Chem. Phys., 38, 540.

Su, ⊂ ., & Quade, C. R. 996, J. Mol. Spectrosc., 175, 390.

Takano, M., Sasada, Y., & Satoh, T. 1968, J. Mol. Spectrosc., 26, 157.

Turner, B. E. 1989, ApJS, 70, 539.

991, ApJS, 76, 617.

Zuckerman, B. et al. 975, ApJ, 196, 199

Ziurys, L. M., & McGonagle, D. 1993, ApJS, 89, 155.

FIGURE CAPTIONS

Fig. 1 --- The potential energy for torsional motion Of the hydroxyl proton in ethanol shown as a function Of torsional angle measured from the *trans* configuration, at which the potential is a minimum. The two different *gauche* wells are equivalent and lie slightly higher in energy than the *trans* well.

Fig. 2. -- Calculated unnormalized wave functions for the lowest-lying *trans* (top), *gauche*+ (middle), and *gauche*- (bottom) torsional substates.

Fig. 3--- Crossings between two selected *gauche*+ and two selected *gauche* - rotational-torsional levels involved in the transitions analyzed here (J(0,J), J(1,J)) with assorted rotational levels of the *trans* substate. Energies relative to the lowest *gauche* rotational-torsional level (*gauche*+ ; J(0,J)) are plotted vs. total angular momentum quantum number J, At the crossings, perturbations which necessitate our current three-state analysis are at their maximum values. For a given series of rotational levels in the *trans* substate, interactions occur either with the *gauche*+ or *gauche*- levels; these possibilities are indicated by + and - respectively in the labelling of the *trans* substate series.

Fig. 4.-- Crossings between two selected *gauche*+ and two selected *gauche* - rotational-torsional levels involved in the transitions analyzed here (J(1,J-1), J(2,J-1)) with assorted rotational levels of the *trans* substate. Energies relative to the lowest *gauche* rotational-torsional level of the four (*gauche*+ ; J(1,J-1)) are plotted vs. total angular momentum quantum number J. At the Crossings, perturbations which necessitate our current three-state analysis are at their maximum values. For a given series Of rotational levels in the

trans substate, interactions recur either with the. *gauche* -i or *gauche* - levels; these possibilities are indicated by + and - respectively in the labelling of the *trans* subtate series.

1 'ig. 5--- Rotat ion diagram for ethanol in Orion-KL using the measured U-lines of Ohishi et al. (1988).

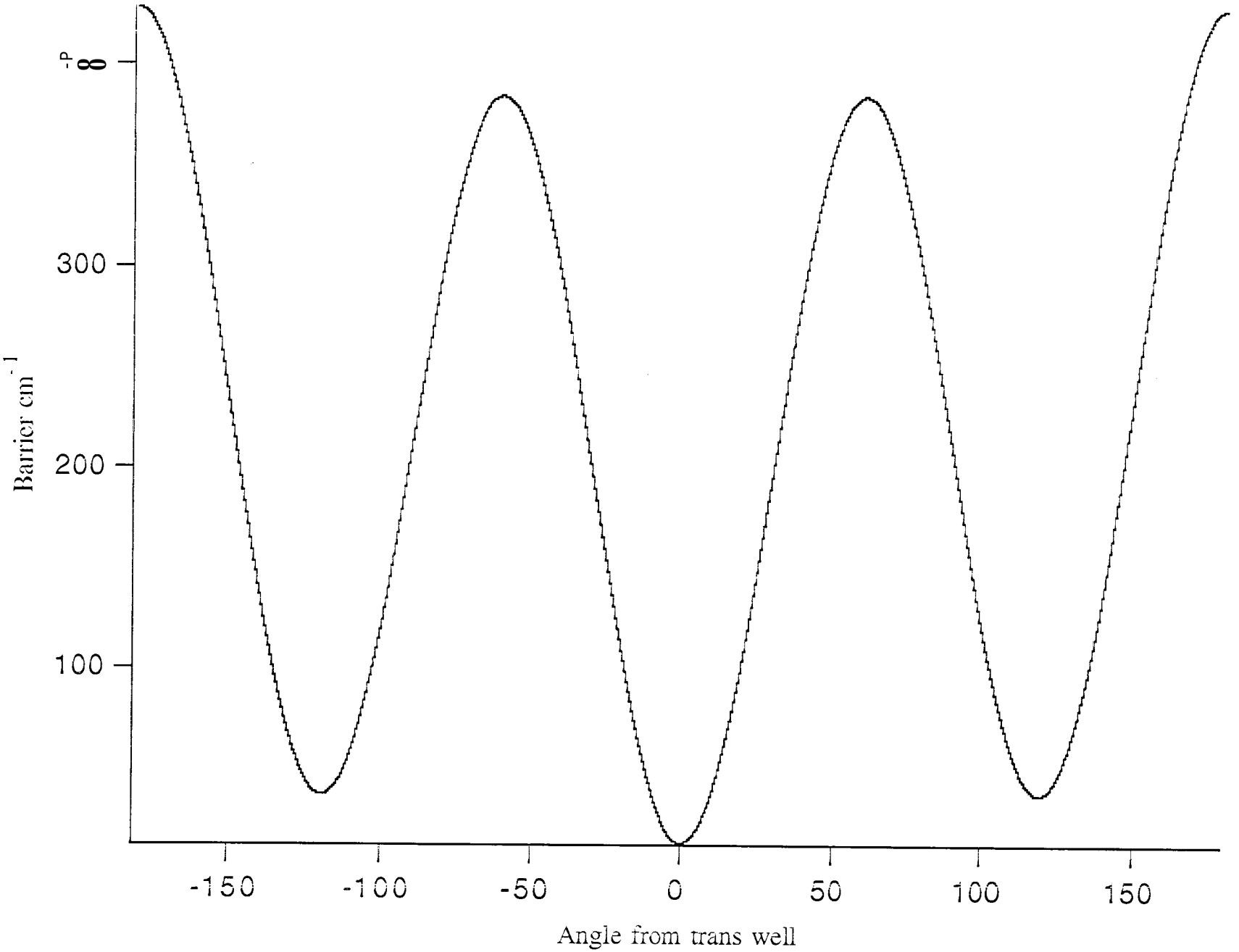
-P
300
200
100
Barrier cm-1
-150
-100
-50
0
50
100
150
Angle from trans well

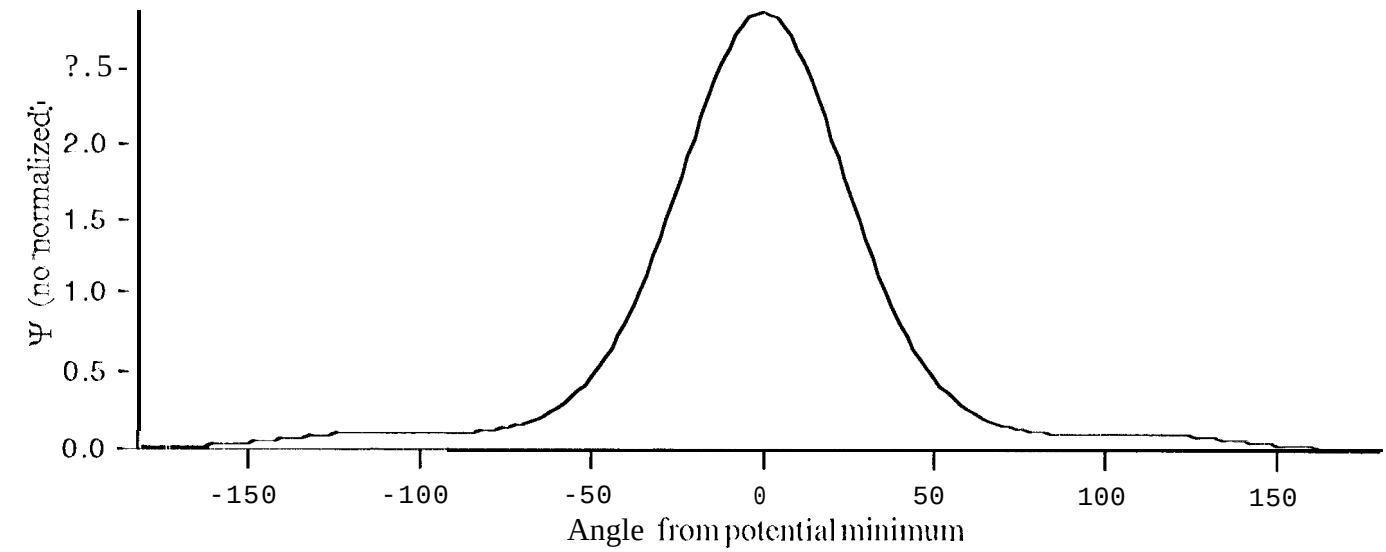
?.5
2.0
1.5
1.0
0.5
0.0
Ψ (no normalized)
-150
-100
-50
0
50
100
150
Angle from potential minimum

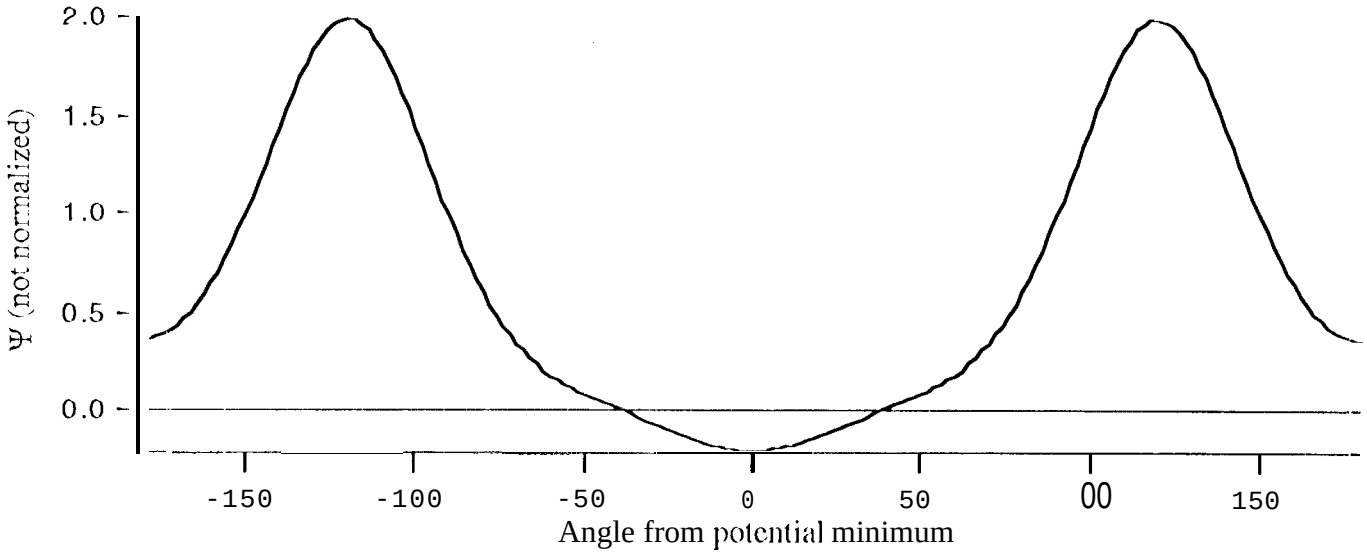
2.0
1.5
1.0
0.5
0.0
Ψ (not normalized)
-150
-100
-50
0
50
00
150
Angle from potential minimum

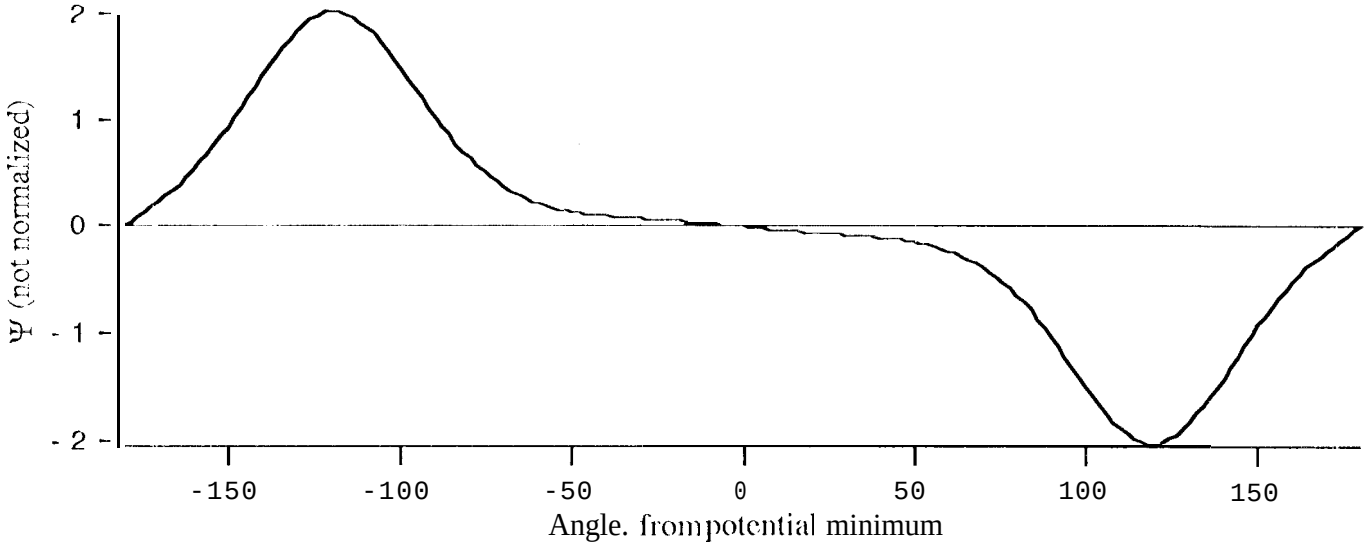
2
1
0
- 1
- 2
Ψ (not normalized)
-150
-100
-50
0
50
100
150
Angle. from potential minimum

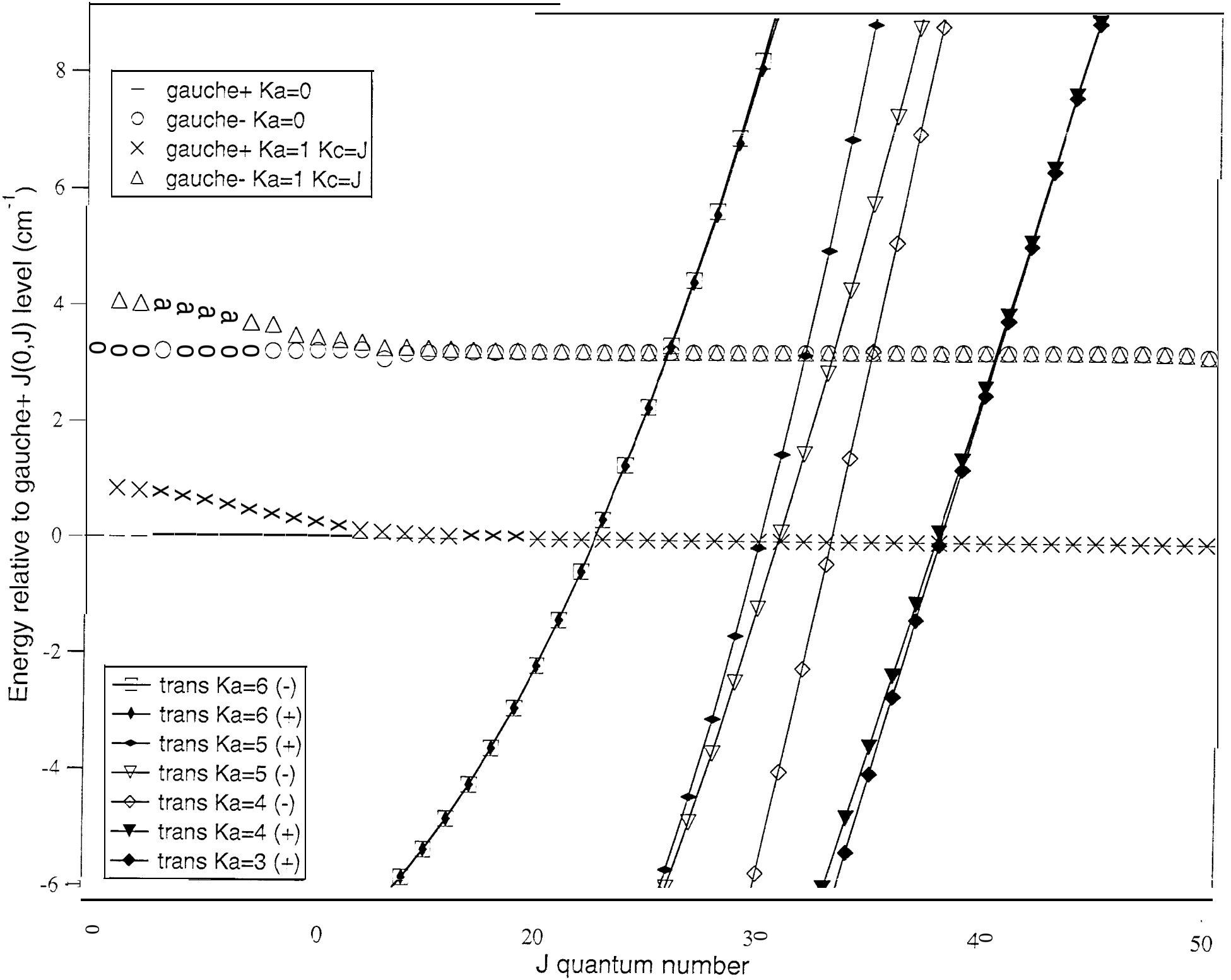
gauche+ Ka=0
gauche- Ka=0
gauche+ Ka=1 Kc=J
gauche- Ka=1 Kc=J
trans Ka=6 (-)
trans Ka=6 (+)
trans Ka=5 (+)
trans Ka=5 (-)
trans Ka=4 (-)
trans Ka=4 (+)
trans Ka=3 (+)
Energy relative to gauche+ J(0,J) level (cm-1)
J quantum number
8
6
4
2
0
-2
-4
-6
0
0
20
30
40
50

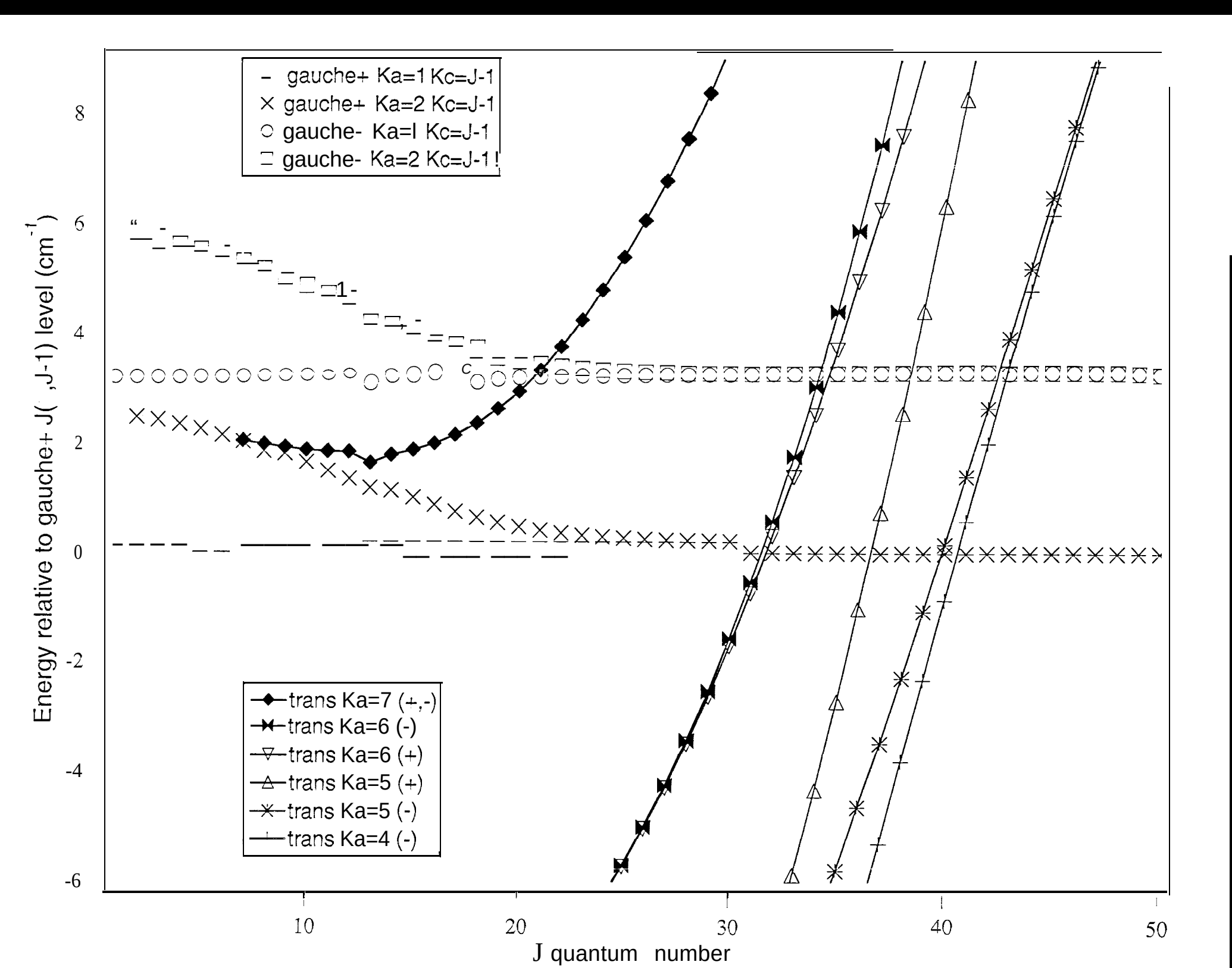
gauche+ Ka=1 Kc=J-1
gauche+ Ka=2 Kc=J-1
gauche- Ka=l Kc=J-1
gauche- Ka=2 Kc=J-1
trans Ka=7 (+,-)
trans Ka=6 (-)
trans Ka=6 (+)
trans Ka=5 (+)
trans Ka=5 (-)
trans Ka=4 (-)
Energy relative to gauche+ J(,J-1) level (cm-1)
J quantum number
8
6
4
2
0
-2
-4
-6
10
20
30
40
50

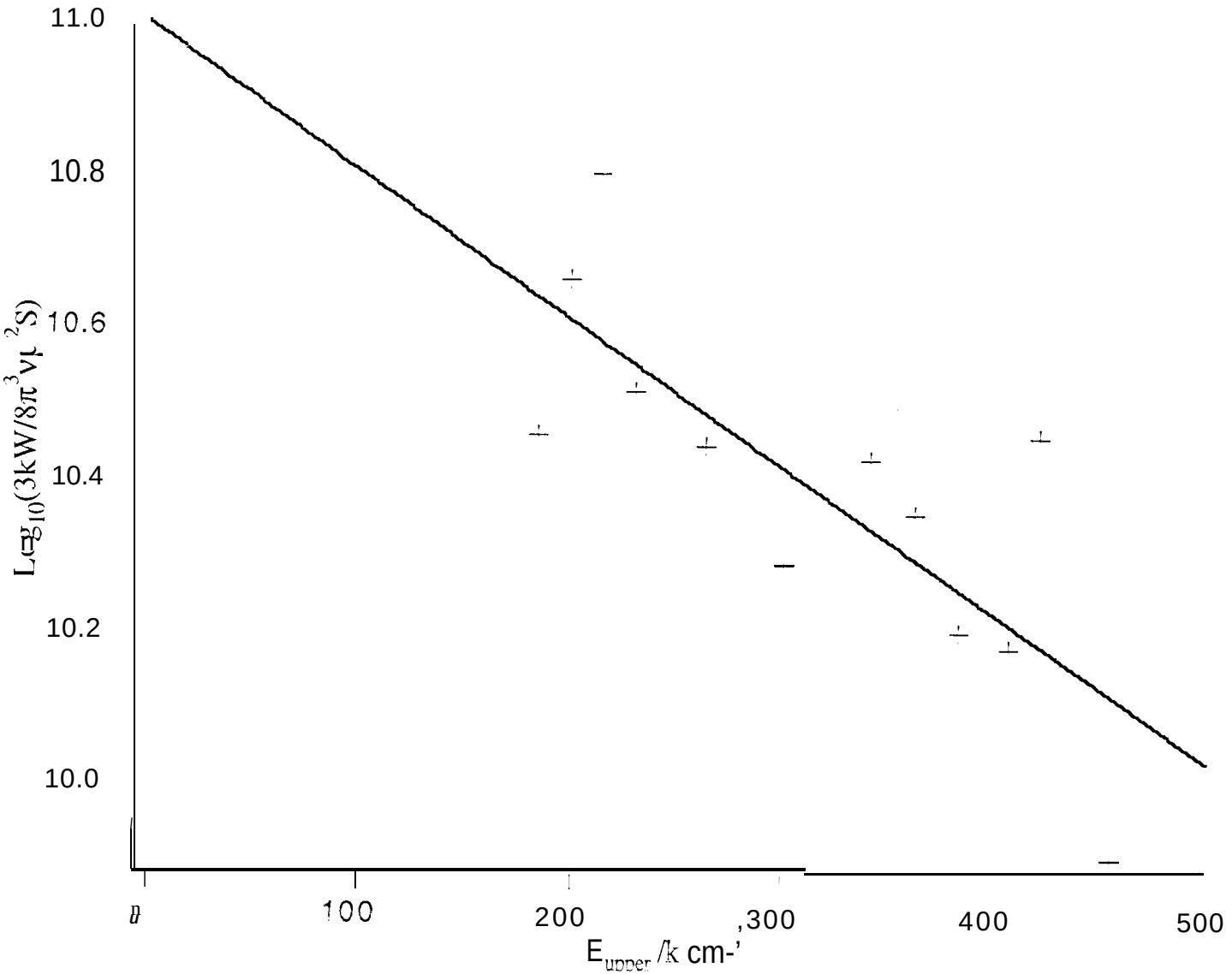
11.0
10.8
10.6
10.4
10.2
10.0
$\mathrm{Log_{10}}(3kW/8\pi^3\nu\mu^2S)$
0
100
200
300
400
500
E_{upper} /k cm-'

TABLE 1

TRANSITION DIPOLE MATRIX

	Trans	Gauche+	Gauche-
Trans	μ_a=0.046 D[a] μ_b=1.438 D[a] μ_c=0.0[c]	μ_a=NA μ_b=NA μ_c=0.0[c]	μ_a=0.0[c] μ_b=0.0[c] μ_c=NA
Gauche+	μ_a=NA μ_b=NA μ_c=0.0[c]	μ_a=1.264 Db μ_b=0.104 D[b] μ_c=0.0[c]	μ_a=0.0[c] μ_b=0.0[c] μ_c=1.101 D[b]
Gauche-	μ_a=0.0[c] μ_b=0.0[c] μ_c=NA	μ_a=0.0[c] μ_b=0.0[c] μ_c=1.101 D[b]	μ_a=1.264 D[b] μ_b=0.104 D[b] μ_c=0.0[c]

NOTE.-- NA=Not available (probably small but fixed to zero in these calculations).

[a] Tanako, Sasada, & Satol (968).

[b] Kakar & Quade (1980).

[c] From symmetry

TABLE 2.

GAUCHE- - GAUCHE+ ^{c}Q AND ^{x}Q BRANCHES WITH K_A=0 OR AND K_C=J

J'K_a K_c	J"K_a"K_c"	Frequency (MHz)	obs-calc (MHz)	log $_{ij}$ ^{a}	E_{lower} (cm^{-1})	notes
1 0 1 1	1 1 1 0	71918.992(50)	-0.420	-5.9464	40.9458	
1 1 1 1	1 0 1 0	121933.986(50)	-0.288	-5.4735	40.1173	
2 0 2 1	2 1 2 0	72986.578(50)	-0.470	-5.6872	42.0628	
2 1 2 1	2 0 2 0	120900.880(50)	-0.279	-5.2632	41.2695	
3 0 3 1	3 1 3 0	74519.642(50)	-0.400	-5.5271	43.7376	
3 1 3 1	3 0 3 0	119420.966(50)	-0.289	-5.1122	42.9949	
4 0 4 1	4 1 4 0	76437.327(50)	-0.378	-5.3712	45.9694	
4 1 4 1	4 0 4 0	117579.752(50)	-0.247	-5.0116	45.2899	
5 0 5 1	5 1 5 0	78637.457(50)	-0.334	-5.2555	48.7569	
5 1 5 1	5 0 5 0	115494.515(50)	-0.220	-4.9332	48.1501	
6 0 6 1	6 1 6 0	81003.969(50)	-0.287	-5.1366	52.0990	
6 1 6 1	6 0 6 0	113325.517(50)	-0.157	-4.8656	51.5703	
7 0 7 1	7 1 7 0	83417.055(50)	-0.237	-5.0434	55.9943	
7 1 7 1	7 0 7 0	111344.327(50)	-0.104	-4.8753	55.5448	
8 0 8 1	8 1 8 0	85765.145(50)	-0.172	-4.9484	60.4413	
8 1 8 1	8 0 8 0	110368.495(50)	-0.051	-4.9570	60.0682	
9 0 9 1	9 1 9 0	87959.044(50)	-0.053	-4.8799	65.4384	
9 0 9 1	9 0 9 0	97034.628(50)	-0.007	-7.0120	65.1357	
9 1 9 1	9 0 9 0	105162.089(50)	-0.172	-4.7503	65.1357	
10 0 10 1	10 1 10 0	89946.985(50)	-0.061	-4.8046	70.9843	
10 0 10 1	10 0 10 0	97159.134(50)	0.052	-6.9866	70.7437	
10 1 10 1	10 1 10 0	96584.856(50)	-0.160	-6.7729	70.9843	
10 1 10 1	10 0 10 0	103796.950(50)	-0.101	-4.7221	70.7437	
11 0 11 1	11 1 11 0	91737.109(50)	0.067	-4.7728	77.0774	gg
11 0 11 1	11 0 11 0	97363.587(50)	0.170	-6.3729	76.8897	gg
11 1 11 1	11 1 11 0	96862.936(50)	-0.137	-6.9448	77.0774	gg
11 1 11 1	11 0 11 0	102489.386(50)	-0.065	-4.6569	76.8897	gg
12 0 12 1	12 1 12 0	93477.574(50)	0.280	-4.7338	83.7165	gg
12 0 12 1	12 0 12 0	97797.282(50)	0.394	-5.9025	83.5724	gg
12 1 12 1	12 1 12 0	97214.225(50)	-0.104	-5.9832	83.7165	gg
12 1 12 1	12 0 12 0	101533.895(50)	-0.028	-4.6726	83.5724	gg
13 0 13 1	13 1 13 0	90007.707(50)	-1.210	-4.9107	90.9003	gg
13 0 13 1	13 0 13 0	93279.005(50)	-1.122	-5.7609	90.7912	gg
13 1 13 1	13 1 13 0	95607.001(50)	0.423	-5.1704	90.9003	gg
13 1 13 1	13 0 13 0	98878.281(50)	0.494	-4.8277	90.7912	gg
14 0 14 1	14 1 14 0	93497.421(50)	-0.780	-4.7021	98.6280	gg
14 0 14 1	14 0 14 0	95946.145(50)	-0.700	-6.3420	98.5463	gg
14 1 14 1	14 1 14 0	96534.856(50)	.072	-6.1002	98.6280	gg
14 1 14 1	14 0 14 0	98983.548(50)	0.121	-4.6196	98.5463	gg
15 0 15 1	15 1 15 0	94696.400(50)	-0.456	-4.6017	106.8985	
15 1 15 1	15 0 15 0	98585.095(50)	0.079	-4.5661	106.8379	
16 0 16 1	16 1 16 0	95416.540(50)	-0.351	-4.6003	115.7111	
16 1 16 1	16 0 16 0	98230.313(50)	0.035	-4.5707	115.6666	
17 0 17 1	17 1 17 0	95924.464(50)	-0.264	-4.5638	125.0652	
17 1 17 1	17 0 17 0	97962.858(50)	0.059	-4.5456	125.0327	
18 0 18 1	18 1 18 0	96301.823(50)	0.198	-4.5669	134.9602	
18 1 18 1	18 0 18 0	97774.307(50)	0.042	-4.5526	134.9367	

'l'All] E 2 *Continued.*

GA UCHE- - GAUCHE+^{c}Q AND ^{x}Q BRANCHES W]'']] K_A=0 OR 1 AND K_C=J

J'K_a'K_c' t.' J"K_a"K_c"t."	Frequency (MHz)	obs - calc 1 og 1	$^{a}E_{lower}$ (cm^{-J})	notes
19 0 19 1 19 1 19 0	96589 .'/ 59(50)	- 0.156	- 4.5464 145.3958	
19 1 19 1 19 0 19 0	97649 .502(50)	0.051	-4.5369 145.3788	
2 0 0 2 0 3 2 0 3 2 0 0	96814.209(50)	- 0.131	-4.5532 156. 3"/15	
2 0 3 2 0 1 2 0 0 2 0 0	9'/574 .042(50)	0.070	-4.5461 156.3593	
21 0 21 1 21 1 21 0	96993.103(50)	- 0.081	-4.5422 16'/ .88'/1	
21 1 21 1 21 0 21 0	97535.908(50)	0.0'27	-4.5373 16"/ .8784	
2 2 0 2 2 1 2 2 1 2 2 0	9'/139 .012(50)	-0.024	-4.5526 1 "/9.9424	
22 1 22 1 22 0 22 0	97525.798(50)	0.060	-4.5490 179.9362	
2 3 0 2 3 1 2 3 1 2 3 0	9"/263 .587,(50)	-0.048	-4.548'/ 192. 53"/0	
2 3 1 2 3 1 2 3 0 2 3 0	9'/536 .849(50)	0.119	-4.5462 192.5326	
24 0 24 1 24 1 24 0	97369 .131 (50)	-0.014	-4.5624 205. 6'/09	
2 4 1 2 4 1 2 4 0 2 4 0	9'/562 .844(50)	0.100	-4.5606 205. 66"/8	
2 5 0 2 5 1 2 5 2 2 5 0	9'/463. '/16(50)	0.023	- 4.5641 '219.3439	
25 1 25 1 25 0 25 0	9'/600 .390(50)	0.085	-4.5629 219.341"/	
26 0 26 1 26 1 26 0	9'/549 .692(50)	0.011	-4.5813 233.5558	
2 6 3 2 6 3 2 6 0 2 6 0	97645.192(50)	0.019	-4.5804 233.5542	
27 o 27 1 27 1 27 o	97631 .329 (50)	0.160	-4.5878 248.3065	
27 1 27 1 27 o 27 o	9"/698 .530(50)	0.056	-4.5872 248.3054	
2 8 0 2 8 3 2 8 1 2 8 0	97'/08 .888(50)	0.114	-4.60'/6 263.5958	
28 1 28 1 28 0 28 0	9"/'/55 .610(50)	0.063	-4.60'/2 263.5950	
29 0 29 1 29 1 29 0	9'/"/ 84.113(50)	0.133	-4.6195 2'/9 .4236	
2 9 1 2 9 1 2 9 0 2 9 0	9'/815.98 "/(50)	0.051	- 4.6192 2"/9 .4231	
30 0 30 1 30 1 30 0	9'/85'/.4'/ 6(50)	0.152	-4.65-/6 295. '/898	tg
3 0 0 3 0 1 3 0 0 3 0 0	97865.529(50)	0.165	-6.0814 295. "/896	tg
30 1 30 1 30 1 30 0	9"/869 .443 (50)	0.169	- 6.0817 295. "/898	tg
30 1 30 1 30 0 30 0	97877 .456(50)	0.056	-4.65-/5 295. "/896	tg
31 1 31 1 31 0 31 0	97998.068(50)	0.021	-4.6928 312.6923	tg
31 1 31 1 31 1 31 0	9'/940. "/33 (50)	0.019	-5.8013 312.6943	tg
3 1 0 3 1 1 3 1 0 3 3 0	9'/989 .809(50)	0.198	-5.8060 312.6923	tg
3 3 0 3 1 1 3 1 1 3 1 0	9'/932 .445(50)	-0.004	-4.6892 312.6943	tg
3 2 2 3 2 1 3 2 0 3 2 0	98021 .302 (50)	0.146	-5.225'/ 330.1.364	tg
3 2 0 3 2 1 3 2 0 3 2 0	98039.493(50)	- 0.031	-4.8335 330.1364	tg
32 1 32 1 32 1 32 0	98006.956(50)	-0.040	-4.8286 330.1369	tg
3 2 0 3 2 1 3 ' 2 1 3 2 0	98025 .13'/ (50)	0.022	-5.232"/ 330.1369	tg
33 1 33 1 33 0 33 0	98091 .922 (50)	0.003	-4. "/5"/0 348. 11'/0	tg
33 0 33 1 33 0 33 0	9808'/ .6'/8 (50)	0.034	- 5.6215 348. 11'/0	tg
33 1 33 1 33 1 33 0	98060.630(250)	0.055	- 5.6233 348.1181	tg B
33 0 33 1 33 1 33 0	98056.249(50)	0.168	- 4. 7581 348.1181	tg
34 1 34 1 34 1 34 0	98163.428(250)	0.042	-4.9232 366. 6354	tg B
3 4 0 3 4 1 3 4 0 3 4 0	98163.428(250)	0.128	-4.9233 366.6353	tg B
34 0 34 1 34 1 34 ()	98160.391 50)	- 0.042	- 5.1'/33 366.6354	tg
34 1 34 1 34 0 34 0	98166.466 50)	0.013	-5.1 "/33 366.6353	tg
35 1 35 1 35 0 35 0	9823"/ .509 50)	0.0'/5	-4.8366 385.6915	tg
35 0 35 1 35 0 35 0	98235 .4'/9 50)	0.021	-5.5059 385.6935	tg
35 1 35 1 35 1 35 0	98236.443 50)	0.025	-5.5059 385.6915	tg
35 0 35 1 35 1 35 0	98234.400 50)	-0.004	-4.8366 385.6915	tg
36 0 36 1 36 1 36 ()	98309.847 50)	- 0.012	-4. '/996 405. 2851	

TABLE 2 *Continued*

GAUCHE- - GA *UCHE*+ ^{c}Q ANI) ^{x}Q BRANCHES WITH I K_A=0 OR 1 ANI) K_C=J

J'K_a'K_c't.'	J"K_a"K_c"t."	Frequency (MHz)	obs - calc 1 og J	^{a} E_{lower} (cm^{-1})	notes
36 1 36 1	36 0 36 0	98322.053(50)	-0.028	-4. "/996 405.2851	
37 o 37 1	37 1 37 O	98386.495(50)	-0.114	-4.8136 425.4160	
37 1 37 1	37 o 37 o	98388.088(50)	-0.105	-4.8136 425.4160	
38 0 38 1	38 1 38 0	98464.381(50)	-0.175	-4.8429 446.0842	
38 1 38 1	38 0 38 0	98465.570(50)	-0.177	-4.8429 446.0842	tg
39 0 39 1	39 1 39 0	98544.249(50)	-0.262	-4.8920 46"/.'2895	tg
39 1 39	1 39 0 39 0	98545.375(50)	-0.29"/	-4.8920 46"/.2895	
40 0 40 1	40 1 40 0	98634.200(50)	-0.583	-4.9859 489.0317	tg
40 1_40 1	40 0 _40 0	98638.544(50)	-0.750	-4.9860 489.031"/	tg

[a] See text: intensity at 300 K.

NOTE. -- B blend; gg *gauche+ gauche-* interaction; tg *trans gauche* int.tract.i on. See also Figure 3.

TABLE 3.

**GA *UCHE*- - GA *UCHE*+ ^{c}Q AN] ^{3}XQ BRANCHES WITH K_A=1 OR 2 AND K_C=J-1

J'Ka'Kc' t'	J"Ka"Kc"t"	Frequency (MHz)	ohs- calc 1 (300) (MHz)	$^{a}E_{lower}$ (cm^{-1})	notes
2 1 1 1	2 2 1 o	22618.680(50)	-0.318	-'/.3022	44.65'13	1
2 2 1 1	2 1 1 0	1"/2641 .532(150)	-0.300	-5.4387	42.1717	2
3 1 2 1	3 2 2 0	24288.620(50)	-0.301	-6.8284	46.386"/	1
3 2 2 1	3 1 2 0	1'/1023 .183(150)	-0.491	-5.2228	43.9554	2
4 1 3 1	4 2 3 0	26501 .'/80 (50)	-0.2'/5	-6. "/6'/7	48.6916	1
4 2 3 1	4 1 3 0	168882.814		-5.0666	46.3321	P
5 1 4 1	5 2 4 0	29255.850(50)	-0. 187	-6.41 67	51.5706	1
5 2 4 1	5 1 4 0	166235 .8'/3 (50)	0.073	-4.9928	49.3005	
6 1 5 1	6 2 5 0	325'/ 0.910(50)	-0.136	-6.4176	55.0214	1
6 2 5 1	6 1 5 0	16310 "/.033		-4.9039	52.8589	P
7 1 6 1	7 2 6 0	36566 .190 (50)	-0.082	-6.0"/16	59.0378	1
7 2 6 1	7 1 6 0	159531.132		-4.8662	5"/.0048	P
8 1 7 1	8 2 7 0	41903.357(50)	-0.011	-6.4575	63.5950	
8 2 7 1	8 1 7 0	155556.341		-4.8091	61 .7354	P
9 1 8 1	9 2 8 0	43196.394(50)	-0.085	-5.9950	68.8693	
9 2 8 1	9 1 8 0	151249.647		-4."/868	67.0470	P
10 1 9 1	10 2 9 0	48378.176(50)	-0.090	-5.7139	"/4.5923	
10 2 9 1	10 1 9 0	246'/06."/63		-4.7587	72.934"/	P
11 1 10 1	11 2 10 0	53529.699(50)	-0.008	-5.5767	80.8901	
11 2 10 1	11 1 10 0	14'2083.013 (50)	0.617	-4."/417	'/9.3916	
12 1 11 1	12 2 11 0	5873"/.6'/8(50)	0.119	-5.4558	87.7546	
12 2 11 1	12 1 11 0	13'/'/49.0"/6(50)	0.927	-4.8002	86.4034	gg
13 1 12 1	13 2 12 0	63952.368(50)	-0.053	-5.3116	95.1823	
13 2 12 1	13 1 12 0	126566.57'/(50)	-0.034	-5.0965	94 .2062	gg
14 1 13 1	14 2 13 0	69108.218(50)	-0.090	-5.2504	103.1705	
14 2 13 1	14 1 13 0	1252'9.125(50)	-0.044	-4.6414	102.2398	gg
15 1 14 1	15 2 14 0	'/4188.188(50)	-0.130	-5.1114	111.7166	
15 2 14 1	15 1 14 0	121496.294(50)	0.211	-4."/000	110.9154	
16 1 15 1	15 2 15 0	'/9364 ."/'/3		-5.15'/6	120.8184	P
16 2 15 1	16 1 15 0	117710.218(50)	0.319	-4.64'/1	120.1491	
17 1 16 1	17 2 16 0	85439.515(50)	-0.153	-5.0884	130.4"/38	gg
17 2 16 1	17 1 16 0	114436.488(50)	0.327	-4."/009	129.9256	
18 1 17 1	18 2 17 0	80605.12(1		-4.9489	140.6806	P gg
18 2 17 1	18 1 17 0	112894.167(50)	0.038	-4.896"7	140.2393	
19 1 18 1	19 2 18 0	84983."/89(50)	-0.193	-4.9370	151.4369	gg
19 2 18 1	19 1 18 0	106931.232(50)	0.436	-4.7099	151.0869	
20 1 19 1	20 2 19 0	88039.2'/6(50)	-0.294	-4."/954	162.7410	
20 2 19 1	20 1 19 0	105225.485(50)	0.424	-4.6364	162.4670	
21 1 20 1	'21 2 20 0	90354.336(50)	-0.404	-4.8119	1'/4.5912	
21 2 20 1	21 1 20 0	103608.598(50)	0.358	-4.6824	1"74.3"/93	
22 1 21 1	22 2 21 0	92156.495(50)	-0.428	-4.'/420	186.9862	
22 2 21 1	22 1 21 0	102282.795(50)	0.317	-4.6499	286.8239	
23 1 22 1	23 2 22 0	93568.906(50)	-0.473	-4."/615	199.9?,47	
23 2 22 1	23 1 22 0	101243.633(50)	0.255	-4.6889	199.8015	

TABLE 3 *Continued.*

GAUCHE- - *GAUCHE+* ^{c}Q AND ^{x}Q BRANCHES WITH K_A=1 OR 2 AND K_C=J-1

J	K_a'	K_c'	t	J"	K_a"	K_c"	t"	Frequency (MHz)	obs-calc (MHz)	J(300)[a]	E_{lower} (cm^{-1})	notes
24	1	23	1	24	2	23	0	94677.029(50)	-0.489	-4.7198	213.4057	
24	2	23	1	24	1	23	0	100452.072(50)	0.213	-4.6677	213.3128	
25	1	24	1	25	2	24	0	95546.737(50)	-0.525	-4.7432	227.4282	
25	2	24	1	25	1	24	0	99864.418(50)	0.162	-4.7032	227.3587	
26	1	25	1	26	2	25	0	96230.704(50)	-0.509	-4.7183	241.9915	
26	2	25	1	26	1	25	0	99440.009(50)	0.097	-4.6894	241.9398	
27	1	26	1	27	2	26	0	96770.969(50)	-0.500	-4.7454	257.0949	
27	2	26	1	27	1	26	0	99143.725(50)	0.055	-4.7237	257.0567	
28	1	27	1	28	2	27	0	97200.941(50)	-0.513	-4.7321	272.7379	
28	2	27	1	28	1	27	0	98946.268(50)	0.005	-4.7164	272.7099	
29	1	28	1	29	2	28	0	97546.875(50)	-0.509	-4.7622	288.9202	
29	2	28	1	29	1	28	0	98823.696(50)	0.000	-4.7507	288.8996	
30	1	29	1	30	2	29	0	97828.953(50)	-0.479	-4.7579	305.6412	
30	2	29	1	30	1	29	0	98755.450(50)	0.026	-4.7497	305.6264	
31	1	30	1	31	2	30	0	98060.635(100)	-0.690	-4.7906	322.9007	B
31	2	30	1	31	1	30	0	98713.724(50)	0.195	-4.7853	322.8907	
32	1	31	1	32	2	31	0	98274.012(50)	0.191	-4.7970	340.6980	
32	1	31	1	32	1	31	0	98614.669(50)	-0.963	-6.8631	340.6866	
32	2	31	1	32	2	31	0	98528.611(50)	0.551	-6.8373	340.6980	
32	2	31	1	32	1	31	0	98869.244(50)	-0.626	-4.7962	340.6866	
33	1	32	1	33	2	32	0	98440.501(50)	-0.156	-4.8301	359.0339	
33	1	32	1	33	1	32	0	98643.608(50)	-0.556	-7.1477	359.0271	
33	2	32	1	33	2	32	0	98624.014(50)	0.188	-7.1414	359.0339	
33	2	32	1	33	1	32	0	98827.119(50)	-0.214	-4.8270	359.0271	
34	1	33	1	34	2	33	0	98602.599(50)	-0.660	-4.8388	377.9074	
34	2	33	1	34	1	33	0	98881.092(50)	-0.001	-4.8358	377.9024	
35	1	34	1	35	2	34	0	98713.078(50)	0.089	-4.8839	397.3186	
35	1	34	1	35	1	34	0	98833.538(50)	-0.150	-6.5377	397.3146	
35	2	34	1	35	2	34	0	98810.614(50)	0.078	-6.5360	397.3186	
35	2	34	1	35	1	34	0	98931.034(50)	-0.201	-4.8817	397.3146	
36	1	35	1	36	2	35	0	98800.965(50)	0.019	-4.9040	417.2683	tg
36	1	35	1	36	1	35	0	98935.903(50)	-0.224	-6.3592	417.2638	tg
36	2	35	1	36	2	35	0	98870.588(50)	0.080	-6.3636	417.2683	tg
36	2	35	1	36	1	35	0	99005.484(50)	-0.206	-4.9016	417.2638	tg
37	1	36	1	37	2	36	0	99091.145(50)	0.231	-5.0904	437.7481	tg
37	1	36	1	37	1	36	0	99033.377(50)	-0.319	-5.4339	437.7500	tg
37	2	36	1	37	2	36	0	99141.023(50)	0.236	-5.4337	437.7481	tg
37	2	36	1	37	1	36	0	99083.254(50)	-0.316	-5.0882	437.7500	tg
38	1	37	1	38	2	37	0	99126.548(50)	-0.168	-4.9950	458.7733	tg
38	1	37	1	38	1	37	0	99145.500(50)	0.056	-5.9168	458.7726	tg
38	2	37	1	38	2	37	0	99162.376(50)	-0.190	-5.9164	458.7733	tg
38	2	37	1	38	1	37	0	99181.326(50)	0.032	-4.9943	458.7726	tg

TABLE 3 *Continued.*

GAUCHE-- GAUCHE+ ^{c}Q AND ^{x}QBRANCHES W]']'}] KA= 1 OR 2 AND KC=J- 1

J'Ka'Kc't' J"Ka"Kc" t"	Frequency (MHz)	obs - calc 1 (300)	^{a} E_{lower} (cm^{-1})	notes
391381392 38 0	9922'/ .093(50)	-0.133	-4.9939	480.3330
391381391 38 0	99242.045(50)	-0.093	-6.80"/6	480.3325
392381392 38 0	99252.987(50)	-0.204	-6.8071	480.3330
392381391 38 0	9926'/.951 (50)	-0.152	-4.9934	480.3325
401391402 39 0	99328.837(50)	-0.'206	-5.0124	50'2.4292
402391401 39 0	99359.033(50)	-0.383	-5.0121	502.4289

[a] See text: intensity at 300 K

NOTES.-- P predicted frequency with 300 kHz uncertainty; B blend; gg *gauche+ gauche-* interaction; tg *trans gauche* interaction. See also Figure 4.

REFERENCES.-- (1) K&Q Kakar and Quade 1980; (2) EAC Cohen 1995.

TABLE 5.

Orion-KL U-LINES ASSIGNED TO *GAUCHE* ETHANOL

U-line (MHz)	Rest Freq (MHz)	T^*_A (K)	Δv (km/s)	$\mu^2 S$ (D^2)	E_{lower} (cm^{-1})	E_{upper} (cm^{-1})	J'Ka'Kc't'	J"Ka"Kc"t"	Notes
U97536.9	97535.908	0.08	4.3	45.60	167.8784	171.1318	21 1 21 1	21 0 21 0	bl
U97536.9	97536.849	0.08	4.3	50.29	192.5326	195.7861	23 1 23 1	23 0 23 0	bl
U97547.3	97546.875	0.06	3.0	48.54	288.9202	292.1740	29 1 28 1	29 2 28 0	
U97550.1	97549.692	0.05	3.9	56.48	233.5558	236.8097	26 0 26 1	26 1 26 0	
U97563.2	97562.844	0.05	2.6	51.78	205.6678	208.9221	24 1 24 1	24 0 24 0	
U97574.7	97574.042	0.09	2.0	42.26	156.3593	159.6140	20 1 20 1	20 0 20 0	
U97597.8	97600.390	0.21	2.7	54.95	219.3417	222.5973	25 1 25 1	25 0 25 0	bl ex
U97632.2	97631.329	0.06	2.9	59.59	248.3065	251.5631	27 0 27 1	27 1 27 0	
U97650.1	97649.502	0.12	2.8	40.88	145.3788	148.6360	19 1 19 1	19 0 19 0	
U97756.4	97755.610	0.05	2.5	61.17	263.5950	266.8558	28 1 28 1	28 0 28 0	
U97774.9	97774.307	0.07	3.2	37.40	134.9367	138.1981	18 1 18 1	18 0 18 0	
U97816.8	97815.987	0.05	2.7	64.11	279.4231	282.6859	29 1 29 1	29 0 29 0	
U97933.1	97932.445	0.06	1.1	63.86	312.6943	315.9610	31 0 31 1	31 1 31 0	
U97963.2	97962.858	0.09	1.5	36.11	125.0327	128.3004	17 1 17 1	17 0 17 0	

NOTES.-- bl = blend; ex = excluded from analysis

TABLE 6.

ADDITIONAL, PROPOSED ASSIGNMENTS

U-line (MHz)	J'Ka'Kc't.'J'Ka"Kc"t"	Rest Freq. (MHz)	T_R/T^*_A (K)	Ref.	Source
U78640	5 0 5 1 5	1 5 0 7863"/ .457	0.05	1	Orion-KL
U90355	21 1 20 1 21	220 0 90354.336	0.08	1	Orion-KL
U97263	23 0 23 1 23	1 23 0 97263.540	0.011		Orion-KL
U98230.2	16 1 16 1 16	0 16 0 98230.313	0.02	2	Orion-KL
U99142	27 2 26 1 27	1 26 0 99143.725	0.10	1	Orion-KL
U100453	24 2 23 1 24	123 0 300452.072	0.0$3	1	Sgr B2
U1 02490	11 1 11 1 11	0 11 0 10.2489.386	0.03	1	Orion-KL
U1 03796	10 1 10 1 10	010 0 103796.950	0.02	1	Orion-KL

REFERENCES.-- (1) Turner 1989; (2) Kutner et al.1980